ARTICLE

Density Functional Theory Study of Finite Carbon Chains

XiaoFeng Fan,[†] Lei Liu,[†,*] JianYi Lin,[‡] ZeXiang Shen,[†] and Jer-Lai Kuo[§]

[†]School of Physical and Mathematical Sciences, Nanyang Technological University, Singapore 637616, [‡]Institute of Chemical & Engineering Sciences, Singapore 627833, and [§]Institute of Atomic and Molecular Sciences, Academia Sinica, Taipei 106, Taiwan

ABSTRACT The structural, electronic, and vibrational properties of the free finite carbon chains and those encapsulated inside carbon nanotubes (CNTs) are studied by density functional theory calculations. The end effect and chain symmetry are found to play key roles in deciding the structural characteristics of the free finite carbon chains based on the parity of the carbon numbers. Due to the potential interaction between the carbon chains and CNTs, the electrons of the chain—CNT systems will redistribute, and some charges may transfer to the inner carbon chains from CNTs. We suggest that the attractive potential of chain atoms inside CNTs could be the driving force for formation of the linear carbon inside CNTs. Unexpectedly, we find that inside CNTs the carbon chains with even-numbered carbons present almost constant bond length alternation, which is independent of the chain length. This trend of the even-numbered carbon chains in CNTs helps to explain the universal experimental observation that the Raman peaks from chains in CNTs are within 1820—1860 cm^{-1}.

KEYWORDS: carbon chain · carbon nanotube · Raman · infrared · density functional theory

CNTs have been intensively studied due to their potential technical applications, including field emission displays, hydrogen storage media, sensors, nanometer-sized semiconductor devices, and so on,[1,2] and their rich physical phenomena,[3] such as possible superconductivity[4] and Peierls distortion.[5−7] A linear carbon chain with pure sp hybridization is expected to hold the promise for atomic-scale field emitting[8,9] and other electronic devices[10,11] and, therefore, enrich further the characteristics and functions of CNTs.[12] However, it was presumed that the cumulated unsaturated bonds of the carbon chain will be reactive and result in the instability under common conditions.[13−17] Being searched experimentally for a long time,[17,18] the isolated linear carbon chains are expected to survive in some protected environments. By high-resolution transmission electron microscopy and resonance Raman spectra, it is confirmed that finite linear chains can be actually stable inside CNTs.[19,20] Thereby, the structural and electronic properties of this new material have attracted many theoretical[21−27] and experimental[28−37] studies, especially on the stability of carbon chains under certain chemical environment.[34] Carbon chains formed with sp-hybridized atoms can be taken as the fourth allotrope of carbon, after diamond, graphite/graphene, and CNTs/fullerenes. Considering the degeneracy of π orbitals of each carbon atom, two forms of infinite carbon chains have been hypothesized.[38] One of the forms, polycumulene, is with the equidistant carbon atoms, whereas the other form, polyyne, is with the alternating single and triple bonds. As the two π orbtials of these sp-hybridized carbons are half occupied, the Peierls distortion will reduce the Fermi energy of electrons by combining the equidistant carbon atoms into conjugated carbon pairs. However, due to the end effect, finite carbon chains may not behave the same as the infinite ones.

In this work, we carry out first-principles density functional theory (DFT) calculations to explore systematically the structural, electronic, and optical properties of finite carbon chains. By considering the end effect and chain symmetry, the different properties between the carbon chains with an odd and even number of carbon atoms are analyzed and explained. Furthermore, we simulate the interaction between the finite carbon chains and single-walled CNTs, where the charge transfer[22] and redistribution between the chain and tube are discussed. Moreover, we demonstrate how the potential field of the carbon chain is reflected by the wall of the CNT and therefore possesses the small delocalized vibration. This may be the reason for the weak interaction and charge transfer between the finite carbon chains and CNTs. Finally, the effects of CNTs on the structural and

*Address correspondence to liulei@ntu.edu.sg.

Received for review August 26, 2009 and accepted October 16, 2009.

Published online October 23, 2009. 10.1021/nn901090e CCC: $40.75

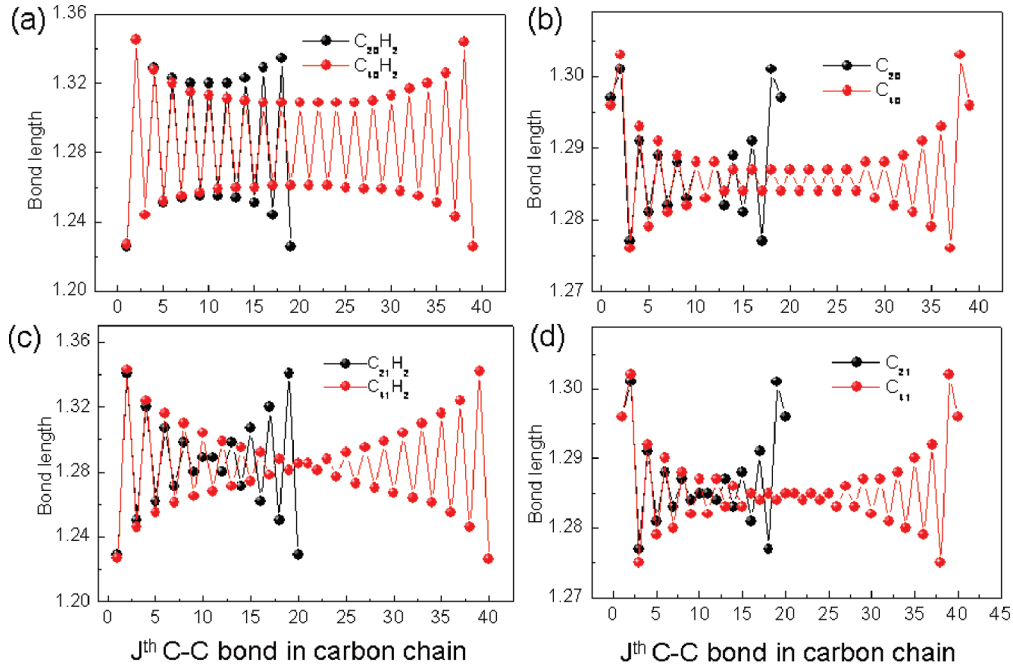

Figure 1. Bond length of all the C−C bonds along the linear chains of $C_{20}H_2$, $C_{40}H_2$, C_{20}, C_{40}, $C_{40}H_2$, $C_{21}H_2$, $C_{41}H_2$,C_{21}, and C_{41}. The bonds starting from one end to the other, numbered as "j".

vibrational properties of the encapsulated finite carbon chains are discussed.

RESULTS AND DISCUSSION

Structural, Electronic, and Vibrational Properties of Free Finite Carbon Chains. For free infinite carbon chains, their optimized structures typically display small bond length alternation (BLA), but for finite carbon chains, the presence of two ends will affect the electronic states of the chain atoms and therefore alter their corresponding stable structures. A series of geometry optimization calculations on chains of C_n and C_nH_2 have been carried out with n from 5 to 52. To elucidate the parity dependence of these linear chains on the number (n) of carbon atoms, the geometries of C_{20}, C_{40}, $C_{20}H_2$, and $C_{40}H_2$ are shown in Figure 1a,b, and the geometries of C_{21}, C_{41}, $C_{21}H_2$, and $C_{41}H_2$ are shown in Figure 1c,d. Two series of BLAs along the chain axis have been observed. For the H-terminated chains, the change of BLAs decays slowly from the end to the center, but without hydrogen termination, the values of BLAs at ends get much bigger and the change of BLAs from the end to center is also distinct. The BLAs of linear chain carbons can be attributed to the Peierls instability of their sp orbitals with the one-dimensional alignment. For the finite carbon chains, the boundary effect will redistribute the charges at ends and enlarge the band length and BLA between carbon atoms accordingly. For the chains without hydrogen termination, the dangling bonds will aggravate this tendency.

From Figure 1, it is interesting to notice that all of the BLAs with odd-numbered carbon atoms approach zero at the chain centers, whereas those with even-numbered carbon atoms are constant. This phenomenon can be explained by considering the center symmetry of the chains. For the even-numbered chain, there are an odd number of bonds and the chain center is on the central bond. For the odd-numbered chain, there are an even number of bonds and the center is at the central atom with two equivalent bonds. Considering the symmetry of the bonds to the center, the lengths of the symmetrically equivalent bonds should be the same. Therefore, the BLA is zero at the center for the odd-numbered chain.

In the infinite carbon chain, the π electrons can be considered as 1D free electron gas with the periodic potential where the Peierls distortion brings the band gap at the edge of the first Brillouin zone (BZ). Obviously, this gap will be folded to the BZ center for the finite carbon chains terminated with certain end atoms. We find that the ends have very strong effect on the electronic states as well as the structures of different length carbon chains. For the chain with an odd number of carbon atoms, the ground electronic state is singlet, whereas for the even-numbered chain, the ground state is triplet. Interestingly, if these carbon chains are terminated by two hydrogen atoms at ends, their ground state tendency is reversed. That is, the chain with an odd number of carbon atoms has the triplet ground state, and the even-numbered chain has the single ground state.

The calculated HOMO−LUMO gaps of the finite chains are found to strongly correlate with the degree of BLA for the chains, as presented in Figure 2. Although the DFT calculations quantitatively underestimate the band gap of molecules, they are expected to predict

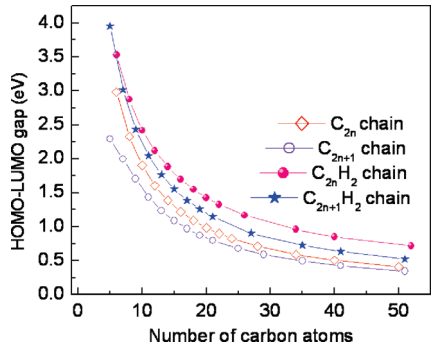

Figure 2. HOMO−LUMO gaps of linear C_n and C_nH_2 chains (n = 5−52).

correctly the variation of the electronic states of the carbon chains in dependence of size. The calculated gaps are found to reduce with the increasing chain size for all four types of chains. This can be mostly attributed to the finite size effect and the end-induced structure variation. As the odd-numbered and even-numbered carbon chains show different changes of BLAs, their HOMO−LUMO gaps show different tendency with atom numbers, as well. The gap difference between C_n and C_nH_2 chains originates from the different dangling bond terminations. The chain $C_{2n}H_2$ with the bigger BLAs and HOMO−LUMO gaps can be very stable, and the isolated $C_{2n}H_2$ chains have even been confirmed experimentally.

The vibrational behaviors of carbon chains are valuable to understand their optical features, such as IR and Raman spectroscopies. For the infinite chain, there are two carbon atoms per unit cell due to Peierls instability, which also results in Kohn anomalies of the optical modes. For those finite chains, the phonon dispersion and Kohn anomalies disappear naturally due to the infinite fold of the Brillouin zone. Then the vibrational modes decided by the free degree of the system become discrete. So there would typically be several optically active modes for each finite carbon chain. As shown in Figure 3, we plot the strongest IR-active mode as the function of the chain sizes for both odd- and even-numbered carbon chains. With the increased size of the chains, the IR-active modes are found to shift to the lower frequency. Similarly, the Raman-active modes

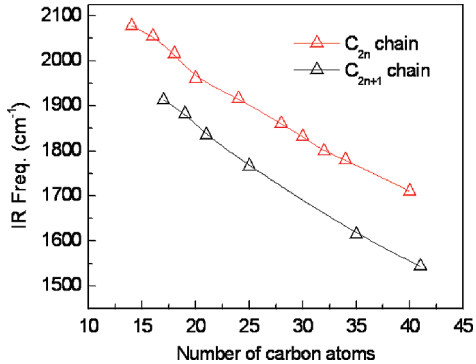

Figure 3. Frequency of the strongest IR peaks as the function of the carbon atom number.

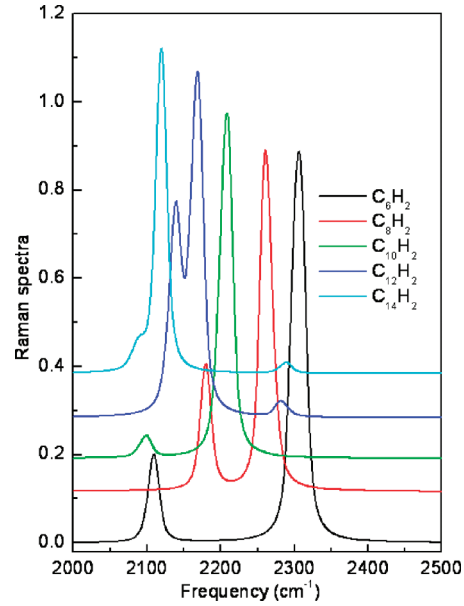

Figure 4. Calculated Raman spectra of C_6H_2, C_8H_2, $C_{10}H_2$, $C_{12}H_2$, and $C_{14}H_2$.

also show red shifts with respect to the chain size. Figure 4 plots the Raman spectra of $C_{2n}H_2$ (n = 3−7), which present a red shift of about 40−50 cm^{-1} per two carbon atoms. The red shifts of these optical modes can be ascribed to the fading of the end effect as the chain length increases.

Finite Carbon Chains Inside CNTs. Usually, a free carbon chain is considered to be unstable and hard to form. Capsulated inside CNTs, the carbon chains will stabilize easily with the protection from the tube walls. Therefore, understanding their formation dynamics and the chain−tube interaction would be meaningful to explore the structural and electronic properties of these CNT-capsulated carbon chains. To illustrate the chemical environment of CNTs, Figure 5 plots the two-dimensional contour of the electrostatic potential

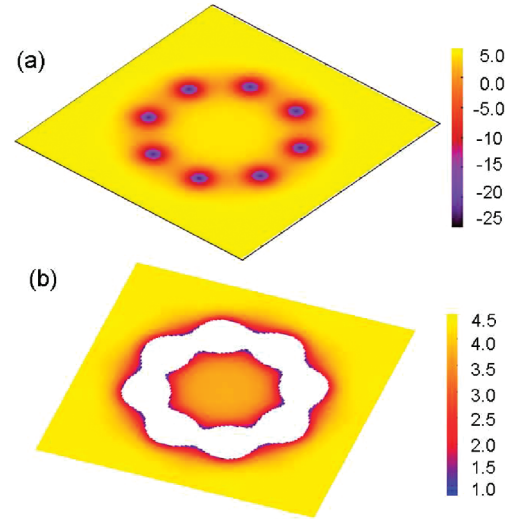

Figure 5. Transverse cross section plot of the calculated electrostatic potential of CNT (8,0) at large (a) and small (b) energy scale.

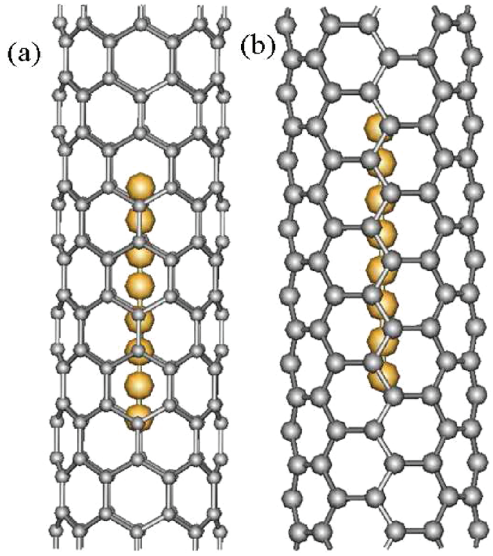

Figure 6. Structures of the C_8 chain inside the 5-unit zigzag (8,0) CNT (a) and the 6-unit armchair (5,5) CNT (b).

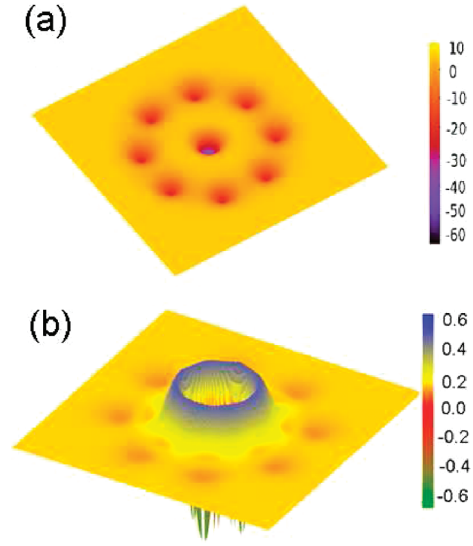

Figure 7. Transverse cross section plot of the calculated electrostatic potential of the chain inside the (8,0) CNT (a) and the calculated potential difference between the chain−CNT system and the independent carbon chain and (8,0) tube (b).

energy of the zigzag (8,0) CNT from the intersection perpendicular to the *z* axis. As shown in Figure 5a, the potentials are very deep along the wall that can trap the carbon π electrons at the local region of the wall. Moreover, there is about 1 eV difference of the potential distribution between the inside and outside of the tube wall, as shown in Figure 5b. We suggest that the relative lower potential inside the CNT walls would be the main driving force to trap the linear carbon chains inside.

The inner diameters of CNTs that contain the carbon chains are found to be 6−7 Å.[19,20] As the distance between the walls and chains is in the range of van der Waals force, this weak force has been taken as the main mechanism of their interaction. Rusznyák *et al.* considered the interaction between the infinite carbon chain and CNTs and concluded that there is charge transfer between them and the two subsystems can establish a common Fermi level.[22] However, some features of this interaction need to be clarified further. For the infinite chain inside the CNT, the incommensurability between the CNT and the chain should be considered. Furthermore, the finite chains may behave differently from the infinite one inside CNTs. Although CNTs can be taken as rigid due to the strong sp^2 bonds, the structures of the inside chains may still be affected by the weak chain−tube interaction. To study the tube−chain interaction effect on the structural and electronic properties of finite carbon chains, without losing generality, we construct two model structures, as shown in Figure 6. One is the supercell (a = 12 Å, b = 12 Å, and c = 21.28 Å) of the semiconducting zigzag (8,0) CNT which is 5 times elongated along the axial direction, and the other is the supercell (a = 14 Å, b = 14 Å, and c = 19.696 Å) of the metallic armchair (5,5) tube which is 6 times elongated axially. In each supercell, a carbon chain of 8 atoms is inserted and the structure is fully optimized.

Figure 7a plots the two-dimensional contour of the electrostatic potential energy from the cross section of the carbon chain inside CNT (8,0) as a representative sample. As the potential distributes locally around the carbon atoms, the chain seemingly presents no interaction with the CNT other than the van der Waals force. Figure 7b plots further the potential difference between the chain−CNT system and the independent carbon chain and CNT. It can be found that the chain−tube combination introduces an additional potential barrier of 0.6 eV between them. This barrier may hinder the charges from transferring from the CNTs to the inside carbon chains. Moreover, some shallow concaves appear between this potential barrier and the CNT carbon atoms. These concaves can be understood as the images of the carbon chain potential reflected from the CNT wall, which may help the charge transfer process. The electrons have been found to transfer from CNTs to the inside finite carbon chains, whether the tube is semiconducting or metallic. The transferred charges can be calculated by the charge difference formula:

$$\Delta CHA(r) = CHA_{CNT-chain}(r) - CHA_{CNT}(r) - CHA_{chain}(r) \quad (1)$$

where $CHA_{CNT-chain}(r)$, $CHA_{CNT}(r)$, and $CHA_{chain}(r)$ are the real space charge distribution of the CNTs with carbon chains inside, the independent CNTs, and carbon chains, respectively. Integrated along the axial *z* axis, the integral distribution of the charge difference in the *x*−*y* plane can be obtained. Figure 8a,b plots the charge difference distributions of the carbon chains within CNT (8,0) and CNT (5,5), respectively. It can be seen clearly that the π electrons of the carbon chains form

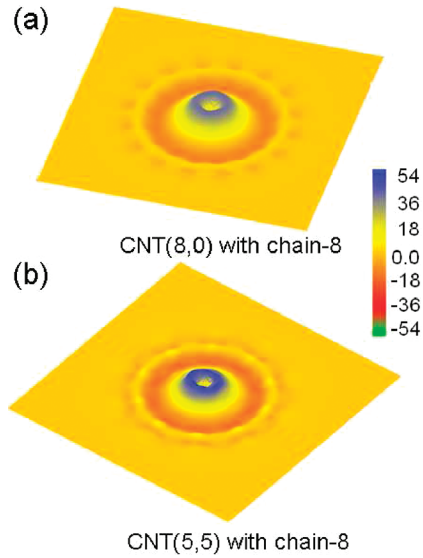

Figure 8. Axial-averaged 2D charge density redistribution (arb. units) of the carbon chain C_8 inside the (8,0) CNT (a) and the (5,5) CNT (b).

a ripple-like fluctuation due to the interaction from the CNT wall. The charge density of the chain atoms redistributes a little bit away from the center as a result of the attraction from the wall atoms, but these charges cannot diffuse far away from the center due to the confinement of the potential barrier, as shown in Figure 7b. Compared with the independent carbon chains and tubes, the chain−tube interaction results in the net charge transfer of about 0.11 electrons per chain carbon atom from the CNTs to the inner carbon chains. By comparing the calculated vibrational spectra of the capsulated chains with the free ones, the charge transfer effect on the vibrational modes of the finite carbon chains has been examined and found to be rather small. Thus, the vibrational behaviors of these carbon chains should be mainly from their bond distributions.

While the charge transfer and redistribution exist, the chain−tube interaction should not be ascribed only to the weak van der Waals force. The relative strong electrostatic force between them will give rise to the structure change of the inner carbon chains, as shown in Figure 9. Induced by the periodic potential fluctuation from the CNTs, the capsulated chains with either an even or an odd number of carbons exhibit much bigger BLAs than the free ones. Furthermore, we find that the BLAs of the chains with even-numbered carbons are almost constant, except for the small variations at the ends. This result indicates that the properties of the even-numbered carbon chains are much like the infinite one, except for the size effect. On the contrary, the capsulated chains with odd-numbered carbons do not have the converged BLAs at the center, such as the C_{11} chain as shown in Figure 9c. Limited by the bond symmetry about the chain center, the odd-numbered chains with the diverged BLAs may possess the higher energy and will be less stable than their

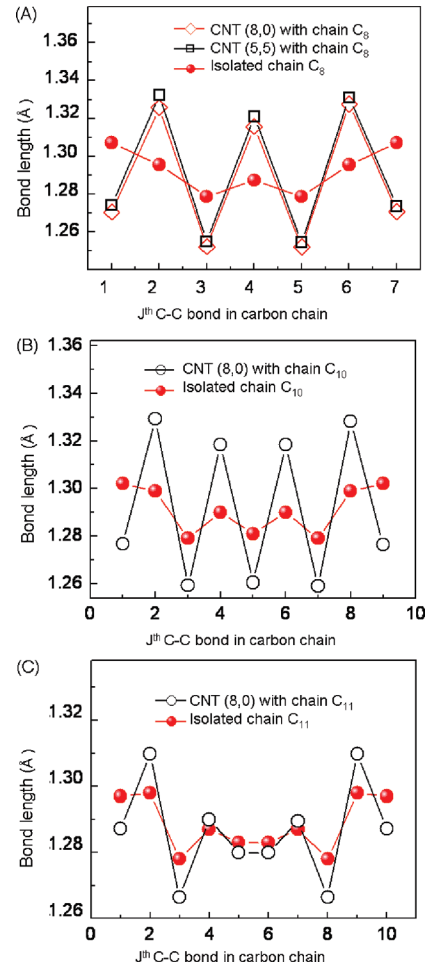

Figure 9. Bond length of the C−C bonds along the linear chains from (a) the free chain C_8, chain C_8 inside CNT (8,0), and chain C_8 inside CNT (5,5), (b) free chain C_{10} and chain C_{10} inside CNT (8,0) and (c) free chain C_{11} and chain C_{11} inside CNT (8,0).

even-numbered counterparts. Therefore, we deduce that the carbon chains capsulated experimentally in CNTs would be most probably with the even-numbered carbon atoms. As the result of the converged BLAs, the optical vibrational modes of the even-numbered capsulated carbon chains will tend to converge rather than to spread over a few hundreds of wavenumbers as the free carbon chains. Therefore, the narrow spectral range of 1820−1860 cm^{-1} of the Raman peaks observed experimentally[20,35−37] on the carbon chains inside CNTs can be understood accordingly.

CONCLUSION

In conclusion, we have performed DFT calculations on the free finite carbon chains and the finite carbon chains capsulated in CNTs. The end effect is found to affect effectively the structural, electronic, and vibrational properties of the free finite carbon chains. These properties of finite chains are also found to be strongly dependent on the size and parity. We notice that the calculated potential inside CNTs is about 1 eV smaller than that outside CNTs, which may be the driving force

for formation of the capsulated linear carbon chains. The calculated charge density distribution of the finite carbon chains inside CNTs indicates that the charge transfer and redistribution characterize these chain−tube systems. Moreover, it is found that the chains with even-numbered carbons will present the constant BLAs inside CNTs. Thus, we may explain clearly why the Raman peaks typically locate within 1820−1860 cm^{-1} in all of the experimental observations so far.

METHODS

In the present work, the calculations of the free carbon chains are performed by using all electron DFT[39,40] at the level of the generalized gradient approximation (GGA) in the Dmol[3] package.[41,42] The Becke exchange with Lee−Yang−Parr correlation functional (BLYP)[43,44] is used to treat the exchange-correlation energy of interacting electrons. The double numerical-polarized basis set (DNP) is employed, and the electron density convergence is set to 1×10^6 e/Å^3. The calculation of vibrational properties is checked with the hybrid DFT method of B3LYP with basis set 6-31G* in the Gaussian 03 package.[45] As molecular orbital codes, Dmol and Gaussian codes can handle the isolated molecules very well. The atomic orbitals are analytically represented by the linear combinations of Gaussian functions in Gaussian 03, but the basis functions are numerically represented on an atomic-centered spherical polar mesh in Dmol[3]. The consistency of the results with different basis sets and exchange-correlation functionals from two packages makes sure that our calculation results are accurate. The interaction between carbon chains and CNTs is simulated using the plane-wave basis VASP code,[46,47] where the projector augmented wave (PAW) method with the GGA-PBE functional is used. Being a plane-wave basis code, VASP would simulate the periodic one-dimensional material of CNTs more efficiently. The kinetic energy cutoff (400 eV) and k-point sampling of the Monkhorst−Pack method[48] are tested to ensure that the total energy converged at the 1 meV/atom. All structures are optimized until the residual forces were smaller than 0.01 eV/Å.

REFERENCES AND NOTES

1. Iijima, S. Helical Microtubules of Graphitic Carbon. *Nature* **1991**, *354*, 56–58.
2. Baughman, R. H.; Zakhidov, A. A.; de Heer, W. A. Carbon Nanotubes—The Route toward Applications. *Science* **2002**, *297*, 787–792.
3. Saito, R., Dresselhaus, G., Dresselhaus, M. S., Eds. *Physical Properties of Carbon Nanotubes*; Imperial College Press: London, 1998.
4. Tang, Z. K.; Zhang, L.; Wang, N.; Zhang, X. X.; Wen, G. H.; Li, G. D.; Wang, J. N.; Chan, C. T.; Sheng, P. Superconductivity in 4 Angstrom Single-Walled Carbon Nanotubes. *Science* **2001**, *292*, 2462–2465.
5. Dubay, O.; Kresse, G.; Kuzmany, H. Phonon Softening in Metallic Nanotubes by a Peierls Like Mechanism. *Phys. Rev. Lett.* **2002**, *88*, 235506.
6. Piscanec, S.; Lazzeri, M.; Robertson, J.; Ferrari, A. C.; Mauri, F. Optical Phonons in Carbon Nanotubes: Kohn Anomalies, Peierls Distortions, and Dynamic Effects. *Phys. Rev. B* **2007**, *75*, 035427.
7. Fouquet, M.; Telg, H.; Maultzsch, J.; Wu, Y.; Chandra, B.; Hone, J.; Heinz, T. F.; Thomsen, C. Longitudinal Optical Phonons in Metallic and Semiconducting Carbon Nanotubes. *Phys. Rev. Lett.* **2009**, *102*, 075501.
8. Derycke, V.; Soukiassian, P.; Mayne, A.; Dujardin, G.; Gautier, J. Carbon Atomic Chain Formation on the β-SiC(100) Surface by Controlled sp→sp^3 Transformation. *Phys. Rev. Lett.* **1998**, *81*, 5868–5871.
9. Rinzler, A. G.; Hafner, J. H.; Nikolaev, P.; Nordlander, P.; Colbert, D. T.; Smalley, R. E.; Lou, L.; Kim, S. G.; Tománek, D. Unraveling Nanotubes: Field Emission from an Atomic Wire. *Science* **1995**, *269*, 1550–1553.
10. Lang, N. D.; Avouris, P. Oscillatory Conductance of Carbon-Atom Wires. *Phys. Rev. Lett.* **1998**, *81*, 3515–3518.
11. Yazdani, A.; Eigler, D. M.; Lang, N. D. Off-Resonance Conduction through Atomic Wires. *Science* **1996**, *272*, 1921–1924.
12. Anantram, M. P.; Léonard, F. Physics of Carbon Nanotube Electronic Devices. *Rep. Prog. Phys.* **2006**, *69*, 507–561.
13. Tománek, D.; Schluter, M. A. Growth Regimes of Carbon Clusters. *Phys. Rev. Lett.* **1991**, *67*, 2331–2334.
14. Jones, R. O. Density Functional Study of Carbon Clusters C_{2n} ($2 \leq n \leq 16$). I. Structure and Bonding in the Neutral Clusters. *J. Chem. Phys.* **1999**, *110*, 5189–5200.
15. Jones, R. O.; Seifert, G. Structure and Bonding in Carbon Clusters C_{14} to C_{24}: Chains, Rings, Bowls, Plates, and Cages. *Phys. Rev. Lett.* **1997**, *79*, 443–446.
16. Ott, A. K.; Rechtsteiner, G. A.; Felix, C.; Hampe, O.; Jarrold, M. F.; Van Duyne, R. P.; Raghavachari, K. Spectra and Calculated Vibrational Frequencies of Size-Selected C_{16} C_{18} and C_{20} Clusters. *J. Chem. Phys.* **1998**, *109*, 9652–9655.
17. Baughman, R. H. Dangerously Seeking Linear Carbon. *Science* **2006**, *312*, 1009–1110.
18. Lagow, R. J.; Kampa, J. J.; Wei, H.-C.; Battle, S. L.; Genge, J. W.; Laude, D. A.; Harper, C. J.; Bau, R.; Stevens, R. C.; Haw, J. F.; Munson, E. Synthesis of Linear Acetylenic Carbon: The "sp" Carbon Allotrope. *Science* **1995**, *267*, 362–367.
19. Wang, Z.; Ke, X.; Zhu, Z.; Zhang, F.; Ruan, M.; Yang, J. Carbon-Atom Chain Formation in the Core of Nanotubes. *Phys. Rev. B* **2000**, *61*, R2472–R2474.
20. Zhao, X.; Ando, Y.; Liu, Y.; Jinno, M.; Suzuk, T. Carbon Nanowire Made of a Long Linear Carbon Chain Inserted Inside a Multiwalled Carbon Nanotube. *Phys. Rev. Lett.* **2003**, *90*, 187401.
21. Liu, Y.; Jones, R. O.; Zhao, X.; Ando, Y. Carbon Species Confined Inside Carbon Nanotubes: A Density Functional Study. *Phys. Rev. B* **2003**, *68*, 125413.
22. Rusznyák, A.; Zólyomi, V.; Kürti, J.; Yang, S.; Kertesz, M. Bond-Length Alternation and Charge Transfer in a Linear Carbon Chain Encapsulated within a Single-Walled Carbon Nanotube. *Phys. Rev. B* **2005**, *72*, 155420.
23. Milani, A.; Tommasini, M.; Zoppo, M. D.; Castiglioni, C.; Zerbi, G. Carbon Nanowires: Phonon and π-Electron Confinement. *Phys. Rev. B* **2006**, *74*, 153418.
24. Tongay, S.; Senger, R.; Dag, S.; Ciraci, S. *Ab-Initio* Electron Transport Calculations of Carbon Based String Structures. *Phys. Rev. Lett.* **2004**, *93*, 136404.
25. Casari, C. S.; Bassi, A. L.; Baserga, A.; Ravagnan, L.; Piseri, P.; Lenardi, C.; Tommasini, M.; Milani, A.; Fazzi, D.; Bottani, C. E.; Milani, P. Low-Frequency Modes in the Raman Spectrum of sp-sp^2 Nanostructured Carbon. *Phys. Rev. B* **2008**, *77*, 195444.
26. Yang, S.; Kertesz, M. Linear C_n Clusters: Are They Acetylenic or Cumulenic? *J. Phys. Chem. A* **2008**, *112*, 146–151.
27. Milani, A.; Tommasini, M.; Zerbi, G. Carbynes Phonons: A Tight Binding Force Field. *J. Chem. Phys.* **2008**, *128*, 064501.
28. Troiani, H. E.; Miki-Yoshida, M.; Camacho-Bragado, G. A.; Marques, M. A. L.; Rubio, A.; Ascencio, J. A.; Jose-Yacaman, M. Direct Observation of the Mechanical Properties of Single-Walled Carbon Nanotubes and Their Junctions at the Atomic Level. *Nano Lett.* **2003**, *3*, 751–755.
29. Cazzanelli, E.; Castriota, M.; Caputi, L. S.; Cupolillo, A.; Giallombardo, C.; Papagno, L. High-Temperature Evolution of Linear Carbon Chains Inside Multiwalled Nanotubes. *Phys. Rev. B* **2007**, *75*, 121405(R).
30. Fantini, C.; Cruz, E.; Jorio, A.; Terrones, M.; Terrones, H.; Lier, G. V.; Charlier, J.-C.; Dresselhaus, M. S.; Saito, R.; Kim, Y. A.;

et al. Resonance Raman Study of Linear Carbon Chains Formed by the Heat Treatment of Double-Wall Carbon Nanotubes. *Phys. Rev. B* **2006**, *73*, 193408.
31. Ravagnan, L.; Piseri, P.; Bruzzi, M.; Miglio, S.; Bongiorno, G.; Baserga, A.; Casari, C. S.; Bassi, A. L.; Lenardi, C.; Yamaguchi, Y.; *et al.* Influence of Cumulenic Chains on the Vibrational and Electronic Properties of sp-sp^2 Amorphous Carbon. *Phys. Rev. Lett.* **2007**, *98*, 216103.
32. Nishide, D.; Wakabayashi, T.; Sugai, T.; Kitaura, R.; Kataura, H.; Achiba, Y.; Shinohara, H. Raman Spectroscopy of Size-Selected Linear Polyyne Molecules $C_{2n}H_2$ ($n = 4-6$) Encapsulated in Single-Wall Carbon Nanotubes. *J. Phys. Chem. C* **2007**, *111*, 5178–5183.
33. Lucotti, A.; Tommasini, M.; Fazzi, D.; Zoppo, M. D.; Chalifoux, W. A.; Ferguson, M. J.; Zerbi, G.; Tykwin, R. R. Evidence for Solution-State Nonlinearity of sp-Carbon Chains Based on IR and Raman Spectroscopy: Violation of Mutual Exclusion. *J. Am. Chem. Soc.* **2009**, *131*, 4239–4244.
34. Jin, C.; Lan, H.; Peng, L.; Suenaga, K.; Iijima, S. Deriving Carbon Atomic Chains from Graphene. *Phys. Rev. Lett.* **2009**, *102*, 205501.
35. Jinno, M.; Bandow, S.; Ando, Y. Multiwalled Carbon Nanotubes Produced by Direct Current Arc Discharge in Hydrogen Gas. *Chem. Phys. Lett.* **2004**, *398*, 256–259.
36. Jinno, M.; Ando, Y.; Bandow, S.; J. Fan, M. Y.; Iijima, S. Raman Scattering Study for Heat Treated Carbon Nanotubes: The Origin of $\approx$1855 cm^{-1} Raman Band. *Chem. Phys. Lett.* **2006**, *418*, 109–114.
37. Cupolillo, A.; Castriota, M.; Cazzanelli, E.; Caputi, L.; Giallombardo, C.; Mariotto, G.; Papagno, L. Second-Order Raman Scattering from Linear Carbon Chains Inside Multiwalled Carbon Nanotubes. *J. Raman Spectrosc.* **2008**, *39*, 147–152.
38. Karpfen, A. *Ab Initio* Studies on Polymers. I. The Linear Infinite Polyyne. *J. Phys. C: Solid State Phys.* **1979**, *12*, 3227–3237.
39. Hohenberg, P.; Kohn, W. Inhomogeneous Electron Gas. *Phys. Rev.* **1964**, *136*, B864–B871.
40. Kohn, W.; Sham, L. J. Self-Consistent Equations Including Exchange and Correlation Effects. *Phys. Rev.* **1965**, *140*, A1133–A1138.
41. Delley, B. An All-Electron Numerical Method for Solving the Local Density Functional for Polyatomic Molecules. *J. Chem. Phys.* **1990**, *92*, 508–517.
42. Delley, B. From Molecules to Solids with the DMol^3 Approach. *J. Chem. Phys.* **2000**, *113*, 7756–7764.
43. Becke, A. D. A Multicenter Numerical Integration Scheme for Polyatomic Molecules. *J. Chem. Phys.* **1988**, *88*, 2547–2553.
44. Lee, C.; Yang, W.; Parr, R. G. Development of the Colle-Salvetti Correlation-Energy Formula into a Functional of the Electron Density. *Phys. Rev. B* **1988**, *37*, 785–789.
45. Frisch, M. J.; Trucks, G. W.; Schlegel, H. B.; Scuseria, G. E.; Robb, M. A.; Cheeseman, J. R.; Montgomery, Jr., J. A.; Vreven, T.; Kudin, K. N.; Burant, J. C. *et al. Gaussian 03*, revision C.02; Gaussian, Inc.: Wallingford, CT, 2004.
46. Kresse, G.; Furthmüller, J. Efficient Iterative Schemes for *Ab Initio* Total-Energy Calculations Using a Plane-Wave Basis Set. *Phys. Rev. B* **1996**, *54*, 11169–11186.
47. Kresse, G.; Joubert, D. From Ultrasoft Pseudopotentials to the Projector Augmented-Wave Method. *Phys. Rev. B* **1999**, *59*, 1758–1775.
48. Monkhorst, H. J.; Pack, J. D. Special Points for Brillouin-Zone Integrations. *Phys. Rev. B* **1976**, *13*, 5188–5192.